AIAA JOURNAL
Vol. 46, No. 3, March 2008

Static Analysis of Sandwich Panels with Square Honeycomb Core

Rakesh K. Kapania,* Hazem E. Soliman,† Summit Vasudeva,† Owen Hughes,‡ and Dhaval P. Makhecha§
Virginia Polytechnic Institute and State University, Blacksburg, Virginia 24061

DOI: 10.2514/1.28121

Static analysis of sandwich panels with a square honeycomb core is performed using the finite element approach applied to the plate theories. The constitutive behavior of an equivalent continuum to the core is obtained using the strain energy approach. The displacement field of the sandwich panel modeled using the equivalent continuum is then compared with results obtained from a highly detailed finite element method created in ABAQUS. The comparison shows the results of the higher-order shear deformation theory in error of 7.6% compared with the detailed model results. An equivalent single layer finite element method for the sandwich panel was then created in ABAQUS and the displacement results of this equivalent single layer model are compared with those obtained from the detailed finite element method. This comparison reveals an error of 6.1% in the results between the two models. A comparison between the equivalent single layer model and the highly detailed model is presented for different core relative densities at two locations of the sandwich panel. A detailed finite element method analysis of the unit cell of the square honeycomb was next performed using ABAQUS and the flexibility approach. Comparison between the equivalent strain energy approach and flexibility approach applied to detailed ABAQUS models of the unit cell proved the equivalent strain energy approach to be efficient.

Nomenclature

C_{ijkl}	=	coefficients of the stiffness matrix
E_c	=	Young's modulus of the material used to manufacture the honeycomb
h_k	=	thickness of the kth layer
u^0	=	x-direction displacement of a point on the midplane of the plate
v^0	=	y-direction displacement of a point on the midplane of the plate
W	=	total strain energy of a unit cell of the square honeycomb
w^0	=	z-direction displacement of a point on the midplane of the plate
w_1, Γ, ξ, ζ	=	functions used in the higher-order shear deformation theory
z_k	=	local transverse coordinate with its origin at the midplane of the kth layer
ε_{ij}	=	strain components
ϕ_x, ϕ_y	=	zigzag functions
ρ_r	=	relative density of the core
ψ_x	=	rotation of the midplane normal about the y axis
ψ_y	=	rotation of the midplane normal about the x axis

Presented as Paper 2168 at the 47th AIAA/ASME/ASCE/AHS/ASC Structures, Structural Dynamics, and Materials Conference, Newport, RI, 1–4 May 2006; received 30 September 2006; revision received 15 July 2007; accepted for publication 10 September 2007.

*Professor, Aerospace and Ocean Engineering Department, 215 Randolph Hall, AIAA Associate Fellow.
†Graduate Research Assistant, Aerospace and Ocean Engineering Department, 215 Randolph Hall, AIAA Student Member.
‡Professor, Aerospace and Ocean Engineering Department, 215 Randolph Hall.
§Former Graduate Research Assistant, Aerospace and Ocean Engineering Department; currently Research Engineer, John F. Welch Technology Center.

I. Introduction

SANDWICH panels have been the focus of numerous studies done in the past few decades due to their high strength to weight ratio and high energy absorption characteristics. The use of sandwich panels is gaining momentum in different industries such as aerospace, automotive, and shipbuilding. Sandwich panels having a honeycomb core constitute the state of the art of lightweight construction due to the amount of weight savings and high strength.

Although it is very important to study the sandwich structures as a whole, it is equally important to analyze the honeycomb core to estimate the material properties of this type of structure to identify its impact on the constitutive behavior. This appears to be the best way in which we can design cores for enhanced energy absorption capability to resist blast and impact loads. The study of the static and dynamic response of honeycomb cores, as well as sandwich panels with other types of cores, has been the focus of many researchers in the past. However, based on an extensive literature study by Noor et al. [1] and to the author's knowledge, studying in detail the complete constitutive behavior of sandwich panels with a honeycomb core has not been attempted theoretically or experimentally.

Many researchers have conducted studies on the properties of honeycomb structures. Torquato et al. [2] conducted a two-dimensional study on the properties of hexagonal, square, and triangular honeycombs. Their study included two approaches, a homogenization approach and a discrete network analysis. Christensen [3] has conducted a two- and three-dimensional study on hexagonal and triangular, a combination of hexagonal and triangular honeycomb, and a combination of hexagonal and star honeycomb structures. Hayes et al. [4] provided simple analytical formulas to obtain the elastic properties of the equivalent continuum to the honeycomb structures based on Timoshenko's beam theory, in addition to some experimental results and provided the response of honeycomb structures to dynamic loading. The idea of using Timoshenko's beam theory, however, to obtain the elastic properties of cellular structures, does not appear to be efficient because it does not represent all the deformations that could be encountered by a cell wall of a honeycomb core. Baker et al. [5] conducted an experimental study on the energy absorption of honeycomb structures made of thick-walled aluminum and stainless steel and having a sinusoidal shape with a straight wall running between every two sinusoidal

waves. Liang and Chen [6] presented the Treble series solution of buckling mode and derived the formulas for determining the critical compressive stress of the square honeycomb. In a series of publications, Papka and Kyriakides [7–10] studied the in-plane compressive response and crushing of honeycombs.

Karagiozova and Yu [11] employed a limit analysis to identify the plastic deformation modes of a hexagonal honeycomb for high thickness to length ratios under in-plane biaxial compression. Other publications [12,13] dealt with that subject as well. Wang and McDowell [14] conducted a study to find the initial yield surfaces of different honeycomb structures including the square and hexagonal honeycomb.

Hohe et al. [15–17] presented a homogenization procedure based on the strain energy equivalence between two bodies if they both have the same response to the same type of loading, subject to the same boundary conditions, and have the same shape with the exception that one of the bodies contains a cellular structure whereas the second body is a continuum. Hohe et al. applied this equivalence to honeycomb structures assuming the existence of an equivalent continuum structure. The determination of the stiffness matrix started by assuming that the deformations in each cell wall of the cellular structure will follow the exact deformation pattern of its edge, i.e., the displacement field is uniform through the depth of the cell wall. Hohe et al. then assumed the edge of the cell wall to deform as a beam. Starting with the displacement field based on Timoshenko's beam theory, Hohe et al. obtained the strains in the cell wall and then assumed a state of plane stress for the cell walls and obtained the stresses in the cell walls using Hooke's law. From the stresses and strains, the strain energy of the entire unit cell is obtained by summing up the strain energy of the individual cell walls. The stiffness matrix is then simply obtained from the strain energy expression. To the authors, the procedure introduced by Hohe et al. is the most recent and most complete as far as obtaining the constitutive behavior of the continuum equivalent to the honeycomb structure is concerned. We point out that developing equivalent continuum is similar to the equivalent plate models that are very prevalent in the aeroelasticity and wing structural analysis (Gern et al. [18], Liu and Kapania [19], Livne et al. [20], and Giles [21]).

In this paper, the constitutive behavior of equivalent continuum to the square honeycomb is obtained using the procedure outlined by Hohe and Becker [17]. We then incorporated the properties obtained in an in-house code that solve sandwich panels to obtain the stress and displacement fields using the finite element (FE) approach applied to the classical laminated plate theory (CLPT) and first-order shear deformation theory (FSDT), as well as the higher-order shear deformation theory (HSDT) [22–26]. For a detailed review of existing theories to analyze complex shear-deformable structures, we refer to the paper by Kapania and Raciti [27].

We also present detailed finite element method (FEM) results for a sandwich panel with a square honeycomb core; these results were obtained using ABAQUS. A comparison between the two procedures shows that the HSDT results are in error of 7.6% compared with the detailed FEM ABAQUS model. We present an equivalent single layer (ESL) finite element method analysis of the sandwich panel with the continuum core equivalent to the square honeycomb that was created in ABAQUS. Comparison of the displacement field results of this model, with respect to the highly detailed FEM of the sandwich panel with a square honeycomb core, shows the ESL model to be in error of 6.1%. Another comparison between the ESL model and the highly detailed model was carried out for different core densities, (10, 15, 20%), at two locations of the sandwich panel, $(0.5L, 0.5L)$ and $(0.25L, 0.25L)$. This comparison shows that the error decreases as the relative density decreases. An investigation of the accuracy of the strain energy approach to calculate the constitutive behavior of the continuum equivalent to the square honeycomb core using detailed ABAQUS models of the unit cells of the square honeycomb is pursued. This investigation proves that the homogenization approach by means of the strain energy equivalence is accurate. We then present simple formulas that correlate the constitutive behavior of a continuum equivalent to the square honeycomb as a function of the relative density of the honeycomb and the elastic modulus of the material used to manufacture the square honeycomb.

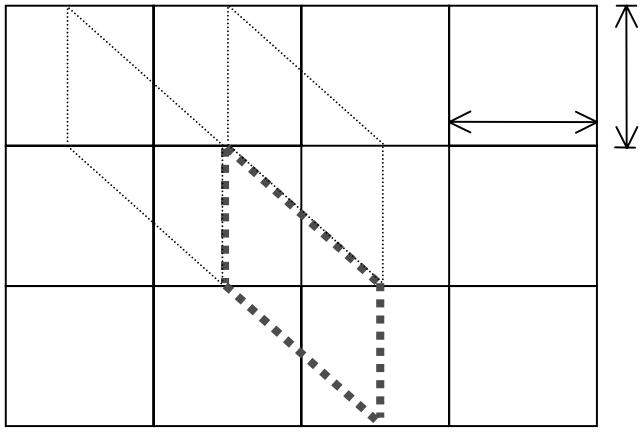

Fig. 1 Representative volume element of the square honeycomb.

II. Strain Energy Approach

The homogenization procedure using the strain energy equivalence approach was developed by Hohe et al. [15–17]. The reader is directed to these references for a complete description of this approach. For brevity and completeness, only a brief review of this procedure applied to the square honeycomb is presented here; more details are offered in Appendix A for the reader's convenience. The approach is based on the fundamental concept that for any volume element containing cellular material, there is an equivalent homogeneous continuum element that has the same strain energy per unit surface area as the cellular structure, provided that both volume elements are subject to the same loading and boundary conditions.

Figure 1 shows an appropriate representative volume element of the square honeycomb. The total strain energy of the volume element is calculated as the sum of the strain energy of the different cell walls contained in this volume element.

The representative volume element of the square honeycomb contains four cell walls. The displacement field for each of the cell walls is assumed to be uniform in the direction normal to the plane of Fig. 1. A Timoshenko beam displacement field is assumed for the cell wall edges shown in Fig. 1. Figure 2 shows the details of breaking up the element into cell walls and the displacement field in the two-dimensional plane of the square honeycomb. The strain field in each cell wall is calculated using the appropriate strain-displacement relations. The stress field is then calculated from the strain field by means of Hooke's law in conjunction with the plane stress assumption in the cell walls. The total strain energy of each cell wall is then calculated as the volume integration of the strain energy density. The coefficients of the stiffness matrix C_{ijkl} are then calculated by differentiating the sum of the total strain energy of all the cell walls in the volume element using the following expression:

$$C_{ijkl} = \frac{\partial^2 W}{\partial \varepsilon_{ij} \partial \varepsilon_{kl}} \tag{1}$$

where W is the sum of the total strain energy of all the cell walls in the volume element.

The constitutive behavior of the continuum equivalent to the square honeycomb is noticed to be identical to transversely isotropic materials.

III. Plate Theories

In this study, the analysis of sandwich panels is carried out using an in-house code that solves sandwich plate problems using the finite element approach applied to the CLT, FSDT and HSDT. In this section, we introduce a comparison between the kinematics of the different plate theories.

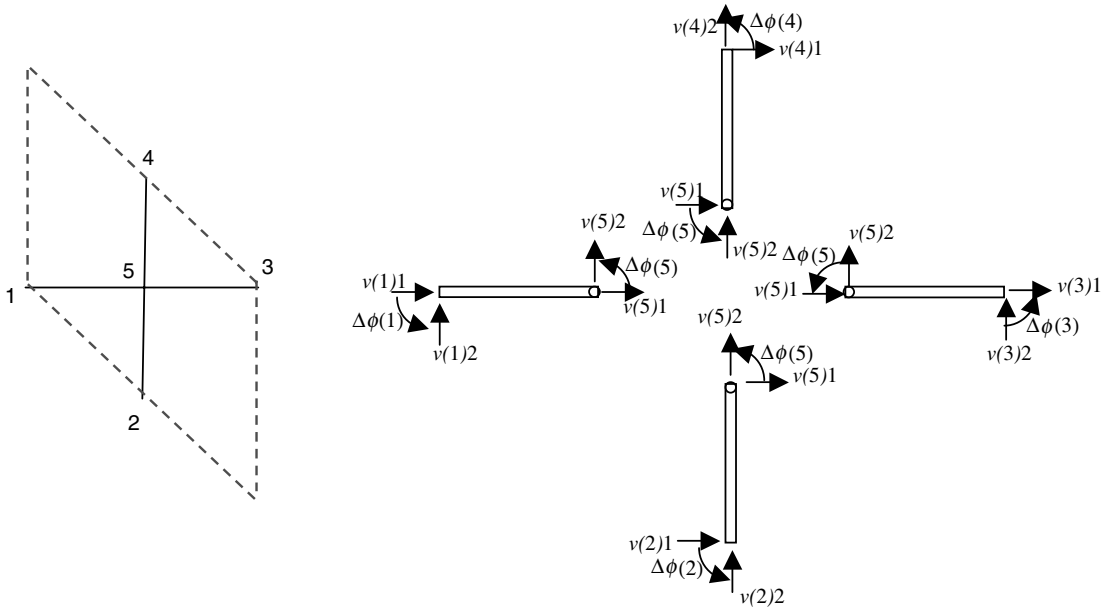

Fig. 2 Square honeycomb element dissected into four cell walls and the assumed displacement field (adapted from Hohe and Becker [17]).

The displacement field in the most general case takes the form

$$\begin{aligned} u(x,y,z) &= u^0(x,y) + z\psi_x(x,y) + z^2\xi_x(x,y) + z^3\varsigma_x(x,y) + S^k\phi_x(x,y) \\ v(x,y,z) &= v^0(x,y) + z\psi_y(x,y) + z^2\xi_y(x,y) + z^3\varsigma_y(x,y) + S^k\phi_y(x,y) \\ w(x,y,z) &= w^0(x,y) + zw_1(x,y) + z^2\Gamma(x,y) \quad S^k = 2(-1)^k z_k/h_k \end{aligned} \tag{2}$$

where $u^0(x, y)$, $v^0(x, y)$, and $w^0(x, y)$ are the displacements of a point (x, y) on the midplane.

The rotations of the midplane normal about the y and x axes are represented by ψ_x, ψ_y, respectively.

The functions w_1, Γ, ξ_x, ξ_y, ζ_x, ζ_y are used only in the HSDT.

The zigzag functions are shown as ϕ_x, ϕ_y.

The local transverse coordinate with its origin at the midplane of the kth layer is z_k.

The thickness of the kth layer is h_k

In the CLPT [20], the normal to the midplane before deformations is assumed to remain straight and normal to the midplane after deformation. This assumption leads to the following:

$$\begin{aligned} &\psi_x = -\frac{\partial w}{\partial x} \qquad \psi_y = -\frac{\partial w}{\partial y} \\ &w_1 = \Gamma = \xi_x = \xi_y = \zeta_x = \zeta_y = \phi_x = \phi_y = 0 \end{aligned} \tag{3}$$

In the FSDT [20], it is assumed that the normal to the midplane before deformation remains straight but not necessarily normal to the midplane after deformation. This assumption leads to the following:

$$\begin{aligned} &\psi_x = \theta_x \qquad \psi_y = \theta_y \\ &w_1 = \Gamma = \xi_x = \xi_y = \zeta_x = \zeta_y = \phi_x = \phi_y = 0 \end{aligned} \tag{4}$$

In the HSDT [22], the in-plane displacements u and v are assumed to have a cubic distribution and, therefore, Eqs. (2) represent the displacement field. In these equations, the functions w_1, Γ, ξ_x, ξ_y, ζ_x, and ζ_y are higher-order terms.

IV. Finite Element Formulations

The derivations of the finite element models for the plate theories used can be found in literature [22–26]. For a review of existing plate and shell elements used for analysis of plates and shells, we refer to the paper by Yang et al. [28]

A brief discussion of the elements is presented here for the reader's convenience. An eight-node serendipity quadrilateral plate element was used for all the FEM analyses. The number of degrees of freedom per node used in the CLPT and FSDT element was five, whereas in the HSDT element, the number was 13. Table 1 lists the degrees of freedom for each of these elements.

The analysis was carried out for a square plate with length $L = 200$ mm. The thickness of the face sheets is 2 mm each, whereas the core thickness is 6 mm. In this analysis, the properties used for the square honeycomb are those obtained for the continuum equivalent to the square honeycomb. Both face sheets and honeycomb core are made of aluminum with Young's modulus of 69 GPa and Poisson's ratio of 0.25. The plate is subject to an out-of-plane pressure of 1 MPa and simply supported boundary conditions on all four sides. The boundary conditions are presented in Eq. (5).

$$\begin{aligned} @x = \pm L/2, \qquad v = 0, \qquad w = 0, \qquad \theta_y = 0 \\ @y = \pm L/2, \qquad u = 0, \qquad w = 0, \qquad \theta_x = 0 \end{aligned} \tag{5}$$

The results obtained for the transverse displacement of the center point of the plate using the finite element approach applied to the CLPT, FSDT and HSDT are then compared with those obtained from a detailed FEM created using ABAQUS. The comparison shows that the HSDT results are in error of 7.6% when compared with the detailed ABAQUS model.

V. ABAQUS Models

A detailed ABAQUS model was created for the sandwich plate with a square honeycomb core. In this model, the square honeycomb core is modeled in great detail, i.e., the cell walls of the square honeycomb are modeled using shell elements; Fig. 3 shows a picture of this plate model with the top and bottom face sheets removed for clarity. In this model, the face sheets and the cell walls of the honeycomb core were modeled using two-dimensional elements in ABAQUS of type S4R5. The plate is simply supported at all four edges. The square plate dimensions are $200 \cdot 200 \cdot 10$ mm and the face sheets are 2 mm thick each, whereas the core is 6 mm thick. The

Table 1 Degrees of freedom used in each of finite element formulations

Theory	Degrees of freedom
CLPT	u^0, v^0, w^0, ψ_x, ψ_y
FSDT	u^0, v^0, w^0, θ_x, θ_y
HSDT	u^0, v^0, w^0, θ_x, θ_y, w_1, Γ, ξ_x, ξ_y, ζ_x, ζ_y, ϕ_x, ϕ_y

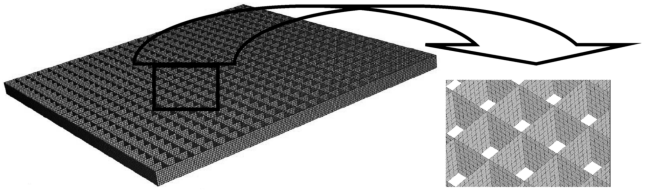

Fig. 3 Detailed ABAQUS model of sandwich plate with square honeycomb core. Face sheets removed for clarity.

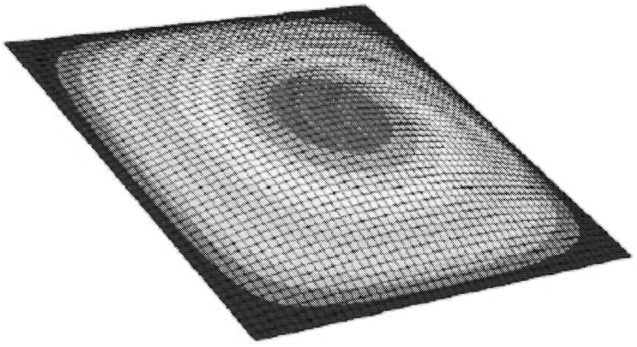

Fig. 4 ABAQUS model of ESL sandwich plate with continuum core.

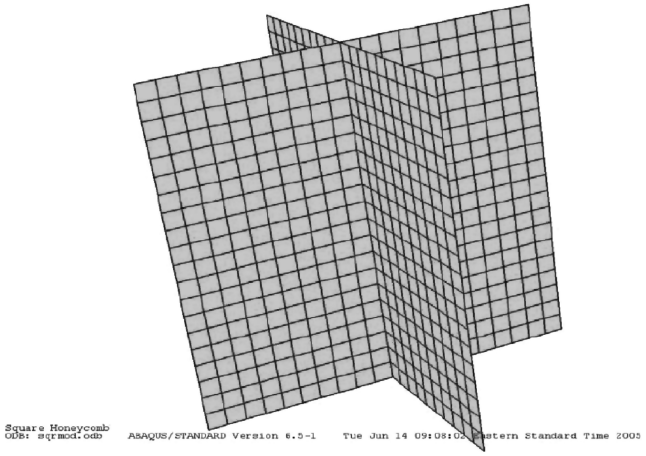

Fig. 5 Finite element model of the unit cell of the square honeycomb using ABAQUS.

element library used in ABAQUS was S4R5 with an element size of $1 \cdot 1$ mm.

An ESL model of the sandwich panel with a continuum core possessing the properties of the square honeycomb obtained via the strain energy approach was created in ABAQUS to evaluate the use of the ESL approach in the analysis of this type of sandwich structure. The library S4R5 of shell elements was used in this model and the panel was subject to the same loads and boundary conditions. The displacement results of this model showed an error of 6.1% when compared with the displacement results obtained from the detailed ABAQUS model of the sandwich panel with the square honeycomb core. Figure 4 shows the ESL model created in ABAQUS for the sandwich panel we are studying. Another comparison between the displacement field obtained using the ESL model and that obtained using the highly detailed FEM was carried out for core relative densities of 10, 15, and 20% at the center point $(0.5L, 0.5L)$ of the plate and at $(0.25L, 0.25L)$. This comparison shows that the error decreases as the relative density decrease.

A detailed ABAQUS model for a unit cell of the square honeycomb was created for the purpose of verifying the accuracy of the strain-energy-based homogenization procedure followed to obtain the properties of the continuum equivalent to the square honeycomb. The unit cell of the square honeycomb was modeled at 20% relative density. Figure 5 shows the FEM of the unit cell created in ABAQUS. The properties were obtained using the flexibility approach applied to this model. The results showed that the strain energy approach followed to obtain the properties of the continuum equivalent to the square honeycomb is highly accurate.

VI. Results

The sandwich structure with a square honeycomb core was studied. The plate dimensions are $200 \cdot 200 \cdot 100$ mm with the thickness of the face sheets taken to be 2 mm each and the core thickness is 6 mm. The plate is subject to an out-of-plane pressure of 1 MPa and simply supported boundary conditions at all four sides. The properties of the continuum equivalent to the square honeycomb core were obtained using a strain-energy-based homogenization approach, in which the strain energy of all the cell walls composing the representative volume element of the square honeycomb are calculated, summed, and differentiated with respect to the strains to obtain the final stiffness matrix of the chosen representative volume element of the square honeycomb. These properties were then incorporated into an in-house code that solves sandwich plate problems using the finite element approach applied to the different plate theories, CLPT, FSDT, and HSDT. The results for the displacement field of the sandwich plate are then obtained.

A detailed finite element model for the sandwich plate was created using ABAQUS; the dimensions, loads, and boundary conditions are same as those used in the aforementioned finite element analysis. In this model, the cell walls of the square honeycomb were modeled using shell elements. The shell elements used in the ABAQUS model were element of type S4R5. The displacement field obtained from this model was then compared with the displacement obtained from the in-house code. This comparison shows that the HSDT is in error of 7.6% with respect to the ABAQUS results, whereas FSDT is in error of 15%, and CLPT is in error of 15.5% with respect to the ABAQUS detailed model.

An ESL model of the sandwich panel with continuum core, possessing the properties of the square honeycomb, obtained using the strain energy approach was created in ABAQUS to evaluate the ESL approach in the analysis of this problem. The displacement field obtained from this model was then compared with the displacement field obtained from the ABAQUS detailed model and the comparison shows that the ESL model results are in error of 6.1% with respect to the ABAQUS detailed model. Table 2 lists the values of the transverse displacement at the center point of the plate for all the analysis techniques mentioned before.

Another comparison was carried out between the displacement field obtained using the ESL model and that obtained using the highly detailed FEM for core relative densities 10, 15, and 20% at $(0.5L, 0.5L)$ and at $(0.25L, 0.25L)$. The results show that the error decreases with an increase in the relative density. These results are listed in Table 3.

The results listed in Tables 2 and 3 led us to investigate the possibility that the homogenization procedure might not be accurate enough to produce the properties of a continuum equivalent to the square honeycomb and a verification of this procedure was needed.

Table 2 Results of the displacement at the center point of the sandwich plate

		Equivalent plate theory		
ABAQUS detailed model S4R5	ABAQUS ESL model S4R5	CLPT	FSDT	HSDT
1.528 mm	1.435 mm	1.291 mm	1.295 mm	1.412 mm

Table 3 Comparison between ESL model and highly detailed FEM

ρ_r	Location	Three-dimensional model	Two-dimensional model, ESL	Error
10%	$(0.5L, 0.5L)$	1.625	1.54	5.2%
	$(0.25L, 0.25L)$	0.8537	0.8435	1.2%
15%	$(0.5L, 0.5L)$	1.56	1.472	5.6%
	$(0.25L, 0.25L)$	0.8002	0.7831	2.1%
20%	$(0.5L, 0.5L)$	1.528	1.435	6.1%
	$(0.25L, 0.25L)$	0.7697	0.744	3.3%

Table 4 Strain energy based approach vs flexibility approach applied using ABAQUS

C_{ijkl}, MPa	Flexibility approach	Strain energy approach	Error
C_{1111}	7360	7360	0%
C_{1122}	0	0	0%
C_{1133}	1840	1840	0%
C_{2222}	7360	7360	0%
C_{2233}	1840	1840	0%
C_{3333}	14260	14720	3.2%
C_{2323}	2748.64	2760	0.4%
C_{1313}	2748.64	2760	0.4%
C_{1212}	37.07	35.94	3%

For this purpose, a detailed finite element model *of the unit cell* of the square honeycomb was created in ABAQUS, the properties of the square honeycomb were found using the flexibility approach applied to this finite element model. Table 4 shows the results obtained for the properties obtained for the continuum equivalent to the square honeycomb using the strain-energy-based homogenization approach against the properties obtained for the square honeycomb by means of the flexibility approach applied to the unit cell of the square honeycomb. The results show that the strain-energy-based approach is highly accurate; in addition, it shows that the square honeycomb behaves as a transversely isotropic material. Another interesting conclusion drawn from these results is that Poisson's ration ν_{12} of the equivalent continuum vanishes.

In an effort to make finding the properties of the continuum equivalent to the square honeycomb easy, the coefficients C_{ijkl} were calculated for the range of relative density between 10–50%. The values for each of the C_{ijkl} normalized by Young's modulus of the material used to manufacture the honeycomb was plotted vs the relative density; the plots show linear variation for all C_{ijkl} except for C_{1212}. Figures 6–10 show these plots, whereas Eqs. (6) represent the corresponding formulas to obtain the coefficients C_{ijkl}.

$$\frac{C_{iiii}}{E_c} = 0.53333\rho_r, \qquad i = 1, 2 \qquad \frac{C_{3333}}{E_c} = 1.06667\rho_r$$
$$\frac{C_{1133}}{E_c} = \frac{C_{2233}}{E_c} = 0.13333\rho_r \qquad \frac{C_{1313}}{E_c} = \frac{C_{2323}}{E_c} = 0.2\rho_r \qquad (6)$$
$$\frac{C_{1212}}{E_c} = 0.0563\rho_r^{2.918}$$

Where ρ_r is the relative density. Young's modulus of the material used to manufacture the square honeycomb is E_c.

VII. Conclusions

The static analysis of sandwich panels with isotropic face sheets and a square honeycomb core was studied. The properties of the continuum equivalent to the square honeycomb core were obtained using a strain-energy-based approach. These properties were then incorporated into an in-house code that solves sandwich panel problems using the finite element method applied to the different plate theories, CLPT, FSDT, and HSDT, and the displacement field was obtained. For verification of the results, a highly detailed ABAQUS model was created for the sandwich panel with a square honeycomb core; in this model, the square honeycomb cell walls were modeled using shell elements. In both cases, the sandwich panel considered was $200 \cdot 200 \cdot 10$ mm, subject to an out-of-plane pressure and simply supported boundary conditions at all four sides of the panel. The comparison between the results for the transverse displacement at the center point of the plate shows that HSDT results are in error of 7.6% compared with the ABAQUS results, whereas CLPT is in error of 15.5%, and FSDT is in error of 15%. An ESL model of the sandwich panel with continuum core possessing the properties of the square honeycomb obtained using the strain-energy-based approach was created in ABAQUS to verify the validity of using the ESL approach in the analysis of this type of sandwich panels. The ESL plate model, having the same dimensions and being subject to the same loading and boundary conditions, was analyzed and the displacement field was obtained. Comparison between the displacement results from the ESL model and the highly detailed model showed that the ESL model is in error of 6.1% with respect to the detailed model. A further investigation of the accuracy of the ESL model compared with the highly detailed FEM was carried out by comparing the displacement field obtained using both approaches for core relative densities 10, 15, and 20%. The results show that the error decreases with the decrease of the relative density.

To investigate the accuracy of the homogenization approach followed to obtain the properties of the continuum equivalent to the

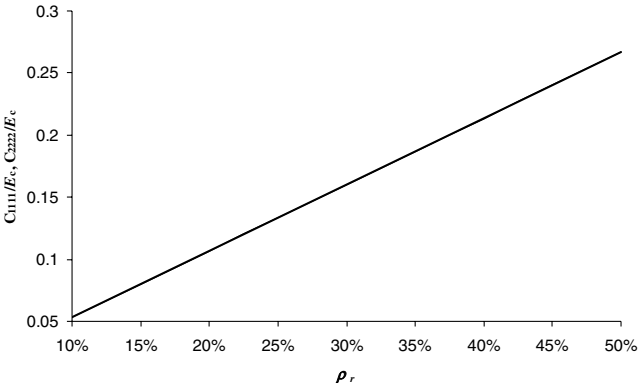

Fig. 6 Variation of C_{1111} and C_{2222} with respect to the relative density.

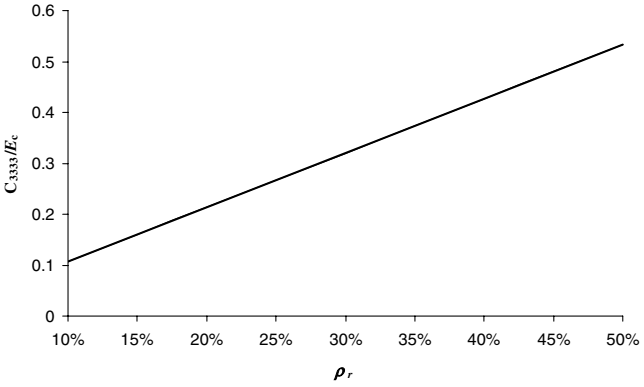

Fig. 7 Variation of C_{3333} with respect to the relative density.

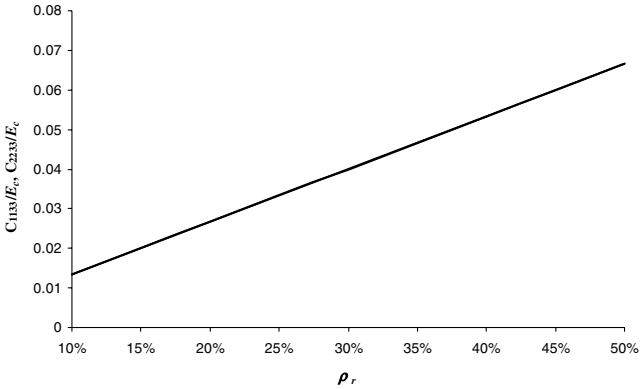

Fig. 8 Variation of C_{1133} and C_{2233} with respect to the relative density.

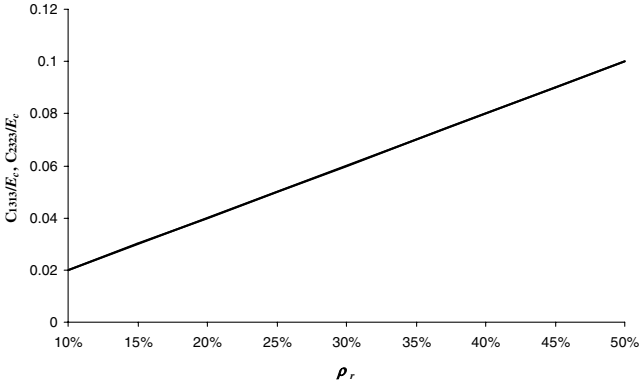

Fig. 9 Variation of C_{1313} and C_{2323} with respect to the relative density.

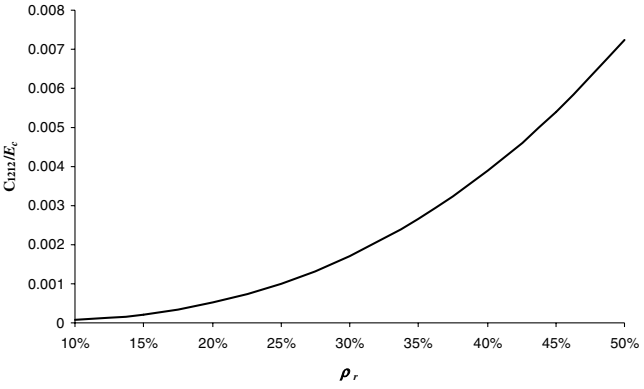

Fig. 10 Variation of C_{1212} with respect to the relative density.

square honeycomb, a detailed ABAQUS model was created for the unit cell of the honeycomb; the properties were then obtained using the flexibility approach applied to the finite element model. The results show a very good agreement between the strain-energy-based homogenization approach and the flexibility approach applied to the finite element model of the unit cell of the square honeycomb. Results of the properties also show that the square honeycomb behaves identically to a transversely isotropic material and all stiffness coefficients vary linearly with the relative density, except for the in-plane shear coefficient.

In this study, due to their widespread use, we have focused on sandwich structures with aluminum face sheets and an aluminum core. Furthermore, the bond between the core and the face sheets is considered to be perfect. We realize that there is an increasing interest in the use of composite face sheets and Nomex core. For such sandwich panels, the effect of material mismatch between the material properties of the face sheets and those of the core would be important and must be studied. However, that was beyond the scope of this study. We are investigating the behavior of material mismatch and the impact of the presence of adhesive layers on the integrity of sandwich panels. A key requirement in such a study would be determination of the interlaminar stresses and material characterization of the adhesives. Interlaminar stresses are often obtained using a postprocessing technique in which the governing equations are integrated directly (Byun and Kapania [29]). The rate-dependent material of adhesives is obtained experimentally and can be used in any commercial code (Makhecha et al. [30]).

Appendix A

Figure 2 shows the representative two-dimensional volume element of the square honeycomb, the dissection of that element into cell walls, and the displacement field.

The total displacement field in a cell wall of length l, thickness t, and height h is assumed to consist of three parts:

1) Homogeneously distributed normal deformation in the x_1–x_3 plane

$$u_1^I(x_i) = v(1)1 + \frac{v(2)1 - v(1)1}{l}x_1$$
$$u_2^I(x_i) = -\frac{\nu}{1-\nu}\left(\frac{v(2)1 - v(1)1}{l} + \varepsilon_{33}\right)x_2 \qquad u_3^I(x_i) = \varepsilon_{33}x_3 \tag{A.1}$$

2) Bending and shear deformation in the x_1–x_3 plane

$$u_1^{II}(x_i) = -\left[\frac{12}{Eht^3}\left(\frac{1}{2}C_1x_1^2 + C_2x_1 + C_3\right) + \frac{l^2\alpha}{Eht^3}C_1\right]x_2$$
$$u_2^{II}(x_i) = \frac{12}{Eht^3}\left(\frac{1}{6}C_1x_1^3 + \frac{1}{2}C_2x_1^2 + C_3x_1 + C_4\right) \qquad u_3^{II}(x_i) = 0 \tag{A.2}$$

where

$$C_1 = \frac{1}{2}Eh\frac{t^3}{l^2}\frac{1}{1+\alpha}\left(-2\frac{v(2)2 - v(1)2}{l} + \Delta\varphi(1) + \Delta\varphi(2)\right)$$
$$C_2 = \frac{1}{12}Eh\frac{t^3}{l}\frac{1}{1+\alpha}\left(6\frac{v(2)2 - v(1)2}{l} - (4+\alpha)\Delta\varphi(1) - (2-\alpha)\Delta\varphi(2)\right)$$
$$C_3 = \frac{1}{12}Eh\frac{t^3}{1+\alpha}\left(\alpha\frac{v(2)2 - v(1)2}{l} + \frac{2+\alpha}{2}\Delta\varphi(1) - \frac{\alpha}{2}\Delta\varphi(2)\right)$$
$$C_4 = \frac{1}{12}Eht^3v(1)2 \qquad \alpha = \begin{cases} \frac{12}{5}(1-\nu)\frac{t^2}{l^2} & \text{Timoshenko theory} \\ 0 & \text{Euler-Bernolli theory} \end{cases}$$

3) Homogeneously distributed transverse shear deformation (x_1–x_3 plane)

$$u_1^{III}(x_i) = 0 \qquad u_2^{III}(x_i) = 0$$
$$u_3^{III}(x_i) = v(1)3 + \frac{v(2)3 - v(1)3}{l}x_1 \tag{A.3}$$

where E and ν in Eqs. (A.1), (A.2), and (A.3) are the elastic constants of the cell material.

The total displacement field is given by $u = u_i^I + u_i^{II} + u_i^{III}$. From the displacement field, the strain field of the cell wall can be obtained by partial differentiation. The stress field is then obtained from the strain field via Hooke's law in conjunction with the plane stress assumption in the cell wall. The strain energy of the cell wall is then obtained as the volume integration of the sum of the products of the components of stress and strain. The result of this process lead to the following:

$$W = \frac{Ehtl}{2(1-\nu^2)}K1 + \frac{1}{(1+\alpha)^2}\left(\frac{t^2}{l^2} + \frac{1}{2}\alpha^2(1-\nu)\right)K2 + \frac{1}{12}\frac{t^2}{l^2}K3 + \frac{1-\nu}{2}K4 \tag{A.4}$$

where

$$K1 = \begin{pmatrix} \frac{v(1)1}{l} \\ \frac{v(2)1}{l} \\ \varepsilon_{33} \end{pmatrix}^T \begin{pmatrix} 1 & -1 & -\nu \\ -1 & 1 & \nu \\ -\nu & \nu & 1 \end{pmatrix} \begin{pmatrix} \frac{v(1)1}{l} \\ \frac{v(2)1}{l} \\ \varepsilon_{33} \end{pmatrix}$$

$$K2 = \begin{pmatrix} \frac{v(1)2}{l} \\ \Delta\phi(1) \\ \frac{v(2)2}{l} \\ \Delta\phi(2) \end{pmatrix}^T \begin{pmatrix} 1 & \frac{1}{2} & -1 & \frac{1}{2} \\ \frac{1}{2} & \frac{1}{4} & -\frac{1}{2} & \frac{1}{4} \\ -1 & -\frac{1}{2} & 1 & -\frac{1}{2} \\ \frac{1}{2} & \frac{1}{4} & -\frac{1}{2} & \frac{1}{2} \end{pmatrix} \begin{pmatrix} \frac{v(1)2}{l} \\ \Delta\phi(1) \\ \frac{v(2)2}{l} \\ \Delta\phi(2) \end{pmatrix}$$

$$K3 = \begin{pmatrix} \Delta\phi(1) \\ \Delta\phi(2) \end{pmatrix}^T \begin{pmatrix} 1 & -1 \\ -1 & 1 \end{pmatrix} \begin{pmatrix} \Delta\phi(1) \\ \Delta\phi(2) \end{pmatrix}$$

$$K4 = \begin{pmatrix} \frac{v(1)3}{l} \\ \frac{v(2)3}{l} \end{pmatrix}^T \begin{pmatrix} 1 & -1 \\ -1 & 1 \end{pmatrix} \begin{pmatrix} \frac{v(1)3}{l} \\ \frac{v(2)3}{l} \end{pmatrix}$$

To determine the nodal deflections, a relation between the stress resultants and the nodal deflections is needed. The stress resultants are obtained by differentiating Eq. (A.4) with respect to the nodal deflections. The result is expressed in matrix form as follows:

$$\begin{pmatrix} \mathbf{F}(1) \\ \mathbf{F}(2) \end{pmatrix} = \begin{pmatrix} \mathbf{K_{11}} & \mathbf{K_{12}} \\ \mathbf{K_{21}} & \mathbf{K_{22}} \end{pmatrix} \begin{pmatrix} v(1) \\ v(2) \end{pmatrix} + \begin{pmatrix} \mathbf{K_{13}} \\ \mathbf{K_{23}} \end{pmatrix} \varepsilon_{33} \tag{A.5}$$

where $\mathbf{F}(i) = [F(i)1, F(i)2, F(i)3, M(i)1]^T$ are the nodal forces and $v(i) = [v(i)1, v(i)2, v(i)3, \Delta\phi(i)]^T$ are the nodal deflections

The stiffness matrices are given as

$$\mathbf{K}_{11} = \frac{Eht}{l(1-\nu^2)} \begin{pmatrix} 1 & 0 & 0 & 0 \\ 0 & \beta & 0 & \beta l/2 \\ 0 & 0 & (1-\nu)/2 & 0 \\ 0 & \beta l/2 & 0 & \left(\frac{\beta l^2}{4} + \frac{t^2}{12}\right) \end{pmatrix}$$

$$\mathbf{K}_{12} = \frac{Eht}{l(1-\nu^2)} \begin{pmatrix} -1 & 0 & 0 & 0 \\ 0 & -\beta & 0 & \beta l/2 \\ 0 & 0 & -(1-\nu)/2 & 0 \\ 0 & -\beta l/2 & 0 & \left(\frac{\beta l^2}{4} - \frac{t^2}{12}\right) \end{pmatrix}$$

$$\mathbf{K}_{21} = \frac{Eht}{l(1-\nu^2)} \begin{pmatrix} -1 & 0 & 0 & 0 \\ 0 & -\beta & 0 & -\beta l/2 \\ 0 & 0 & -(1-\nu)/2 & 0 \\ 0 & \beta l/2 & 0 & \left(\frac{\beta l^2}{4} - \frac{t^2}{12}\right) \end{pmatrix}$$

$$\mathbf{K}_{22} = \frac{Eht}{l(1-\nu^2)} \begin{pmatrix} 1 & 0 & 0 & 0 \\ 0 & \beta & 0 & -\beta l/2 \\ 0 & 0 & (1-\nu)/2 & 0 \\ 0 & -\beta l/2 & 0 & \left(\frac{\beta l^2}{4} + \frac{t^2}{12}\right) \end{pmatrix}$$

$$\begin{pmatrix} \mathbf{K_{13}} \\ \mathbf{K_{23}} \end{pmatrix} = \frac{Eht}{l(1-\nu^2)} (-l\nu \quad 0 \quad 0 \quad l\nu \quad 0 \quad 0)^T$$

The aforementioned relations provide a linear system of equations, the solution of which provides the nodal deflections of the entire volume element.

Acknowledgment

The authors gratefully acknowledge the Office of Naval Research for their financial support for this research.

References

[1] Noor, A. K., Burton, W. S., and Bert, C. W., "Computational Models for Sandwich Panels and Shells," *Applied Mechanics Reviews*, Vol. 49, No. 3, 1996, pp. 155–199.

[2] Torquato, S., Gibiansky, L. V., Silva, M. J., and Gibson, L. J., "Effective Mechanical and Transport Properties of Cellular Solids," *International Journal of Mechanical Sciences*, Vol. 40, No. 1, 1998, pp. 71–82. doi:10.1016/S0020-7403(97)00031-3

[3] Christensen, R. M., "Mechanics of Cellular and Other Low-Density Materials," *International Journal of Solids and Structures*, Vol. 37, No. 1, 2000, pp. 93–104. doi:10.1016/S0020-7683(99)00080-3

[4] Hayes, A. M., Wang, A., Dempsey, B. M., and McDowell, D. L., "Mechanics of Linear Cellular Alloys," *Mechanics of Materials*, Vol. 36, No. 8, 2004, pp. 691–713. doi:10.1016/j.mechmat.2003.06.001

[5] Baker, W. E., Togami, T. C., and Weydert, J. C., "Static and Dynamic Properties of High-Density Metal Honeycombs," *International Journal of Impact Engineering*, Vol. 21, No. 3, 1998, pp. 149–163. doi:10.1016/S0734-743X(97)00040-7

[6] Liang, S., and Chen, H. L., "Investigation on the Square Cell Honeycomb Structures Under Axial Loading," *Composite Structures*, Vol. 72, No. 4, 2006, pp. 446–454. doi:10.1016/j.compstruct.2005.01.022

[7] Papka, S. D., and Kyriakides, S., "Biaxial Crushing of Honeycombs, Part 1: Experiments," *International Journal of Solids and Structures*, Vol. 36, No. 29, 1999, pp. 4367–4396. doi:10.1016/S0020-7683(98)00224-8

[8] Papka, S. D., and Kyriakides, S., "In-Plane Biaxial Crushing of Honeycombs, Part 2: Analysis," *International Journal of Solids and Structures*, Vol. 36, No. 29, 1999, pp. 4397–4423. doi:10.1016/S0020-7683(98)00225-X

[9] Papka, S. D., and Kyriakides, S., "In-Plane Compressive Response and Crushing of Honeycomb," *Journal of the Mechanics and Physics of Solids*, Vol. 42, No. 10, 1994, pp. 1499–1532. doi:10.1016/0022-5096(94)90085-X

[10] Papka, S. D., and Kyriakides, S., "In-Plane Crushing of Polycarbonate Honeycomb," *International Journal of Solids and Structures*, Vol. 35, Nos. 3–4, 1998, pp. 239–267. doi:10.1016/S0020-7683(97)00062-0

[11] Karagiozova, D., and Yu, T. X., "Plastic Deformation Modes of Regular Hexagonal Honeycombs Under In-Plane Biaxial Compression," *International Journal of Mechanical Sciences*, Vol. 46, Oct. 2004, pp. 1489–1515. doi:10.1016/j.ijmecsci.2004.09.010

[12] Mcfarland, R. K., Jr., "Hexagonal Cell Structures Under Post-Buckling Axial Load," *AIAA Journal*, Vol. 1, No. 6, 1963, pp. 1380–1385.

[13] Cote, F., Deshpande, V. S., Fleck, N. A., and Evans, A. G., "The Out-of-Plane Compressive Behavior of Metallic Honeycombs," *Materials Science and Engineering A*, Vol. 380, Nos. 1–2, Aug. 2004, pp. 272–280. doi:10.1016/j.msea.2004.03.051

[14] Wang, A. J., and McDowell, D. L., "Yield Surfaces of Various Periodic Metal Honeycombs at Intermediate Relative Density," *International Journal of Plasticity*, Vol. 21, No. 2, Feb. 2005, pp. 285–320. doi:10.1016/j.ijplas.2003.12.002

[15] Hohe, J., and Becker, W., "Effective Elastic Properties of Triangular Grid Structures," *Composite Structures*, Vol. 45, No. 2, 1999, pp. 131–145. doi:10.1016/S0263-8223(99)00016-1

[16] Hohe, J., Beschorner, C., and Becker, W., "Effective Elastic Properties of Hexagonal and Quadrilateral Grid Structures," *Composite Structures*, Vol. 46, No. 1, 1999, pp. 73–89. doi:10.1016/S0263-8223(99)00048-3

[17] Hohe, J., and Becker, W., "An Energetic Homogenization Procedure for the Elastic Properties of General Cellular Sandwich Cores," *Composites. Part B, Engineering*, Vol. 32, No. 3, 2001, pp. 185–197. doi:10.1016/S1359-8368(00)00055-X

[18] Gern, F. H., Inman, D. J., and Kapania, R. K., "Structural and Aeroelastic Modeling of General Planform UCAV Wings with Morphing Airfoils," *AIAA Journal*, Vol. 40, No. 4, April 2002, pp. 628–637.

[19] Liu, Y., and Kapania, R. K., "Equivalent Skin Analysis of Wing Structures Using Neural Networks," *AIAA Journal*, Vol. 39, No. 7, July 2001, pp. 1390–1399.

[20] Livne, E., Sels, R. A., and Bhatia, K. G., "Lessons from Application of Equivalent Plate Structural Modeling to an HSCT Wing," *Journal of Aircraft*, Vol. 31, No. 4, 1994, pp. 953–960.

[21] Giles, G. L., "Equivalent Plate Analysis of Aircraft Wing Box Structures With General Platform Geometry," *Journal of Aircraft*, Vol. 23, No. 11, 1986, pp. 859–864.

[22] Makhecha, D. P., Patel, B. P., and Ganapathi, M., "Transient Dynamics of Thick Skew Sandwich Laminates Under Thermal/Mechanical Loads," *Journal of Reinforced Plastics and Composites*, Vol. 20, No. 17, 2001, pp. 1524–1545.
doi:10.1177/073168401772679129

[23] Timoshenko, S. P., and Goodier, J. N., *Theory of Elasticity*, 3rd ed., McGraw–Hill, New York, 1951.

[24] Reddy, J. N., *Mechanics of Laminated Composite Plates and Shells: Theory and Analysis*, 2nd ed., CRC Press, Boca Raton, FL, 2004.

[25] Ren, J. G., and Hinton, E., "The Finite Element Analysis of Homogeneous and Laminated Composite Plates Using a Simple Higher Order Theory," *Communications in Applied Numerical Methods*, Vol. 2, No. 2, 1986, pp. 217–228.
doi:10.1002/cnm.1630020214

[26] Ganapathi, M., Patel, B. P., and Makhecha, D. P., "Nonlinear Dynamic Analysis of Thick Composite/Sandwich Laminates Using an Accurate Higher-Order Theory," *Composites. Part B, Engineering*, Vol. 35, No. 4, 2004, pp. 345–355.
doi:10.1016/S1359-8368(02)00075-6

[27] Kapania, R. K., and Raciti, S., "Recent Advances in Analysis of Laminated Beams and Plates, Part 1: Shea Effects and Buckling," *AIAA Journal*, Vol. 27, No. 7, 1989, pp. 923–934.

[28] Yang, T. Y., Saigal, S., Masoud, A., and Kapania, R. K., "Advances in Shell Finite Element Computations," *International Journal for Numerical Methods in Engineering*, Vol. 47, Nos. 1–32000, pp. 101–127.
doi:10.1002/(SICI)1097-0207(20000110/30)47:1/3<101::AID-NME763>3.0.CO;2-C

[29] Byun, C., and Kapania, R. K., "Prediction of Interlaminar Stresses in Laminated Plates Using Global Orthogonal Interpolation Polynomials," *AIAA Journal*, Vol. 30, No. 11, 1992, pp. 2740–2749.

[30] Makhecha, D. P., Kapania, R. K., Johnson, E. R., and Dillard, D. A., Implementation of the Cohesive Zone Model in a Explicit Code (LS-DYNA) Through a User Defined Material Model to Study High Speed Crack Growth," AIAA Paper 2006-1961, 2006; *AIAA Journal* (under revision).

B. Balachandran
Associate Editor